Digital Communications and Networks 3 (2017) 1–10

HOSTED BY

ELSEVIER

Contents lists available at ScienceDirect

Digital Communications and Networks

journal homepage: www.elsevier.com/locate/dcan

On distributed power control in full duplex wireless networks[☆]

Yu Wang, Shiwen Mao[*]

Department of Electrical and Computer Engineering, Auburn University, Auburn, AL, USA

ARTICLE INFO

Keywords:
Dual decomposition
Distributed algorithm
Full duplex transmission
Power control

ABSTRACT

In this paper, we first consider the problem of distributed power control in a Full Duplex (FD) wireless network consisting of multiple pairs of nodes, within which each node needs to communicate with its corresponding node. We aim to find the optimal transmition power for the FD transmitters such that the network-wide capacity is maximized. Based on the high Signal-to-Interference-Plus-Noise Ratio (SINR) approximation and a more general approximation method for logarithm functions, we develop effective distributed power control algorithms with the dual decomposition approach. We also extend the work to the general FD network scenario, which can be decomposed into subproblems of isolated nodes, paths, and cycles. The corresponding power control problem is then be solved with the distributed algorithm. The proposed algorithms are validated with simulation studies.

1. Introduction

Due to the broadcast nature of wireless transmissions, a receiver is usually interfered by undesired signals that it overhears from neighboring transmitters. The capacity of a wireless network is mainly limited by interference. Consider people chatting at a party. In order to be heard clearly, one may want to enlarge their voice. However, if everyone tries to do so, they will end up shouting at the top of their voices, but, unfortunately, still get bad reception. To this end, a Medium Access Control (MAC) protocol is used to exclude transmission within a footprint centered at the receiver. Alternatively, an effective power control scheme can be used to find the optimal transmitting powers for the transmitters, such that the network capacity is maximized [1,2].

In this paper, we investigate the problem of distributed power control for a wireless network where the nodes are capable of Full Duplex (FD) transmissions. Although FD transmission has been used in wired networks for years (e.g., Asymmetric Digital Subscriber Line (ADSL) based on echo cancellation), FD transmission in wireless networks has become feasible only in recent years. Wireless FD systems are made possible by breakthroughs in self-interference cancellation [3,4], such as Propagation-Domain Suppression (PDIS) [5,6], analog-domain interference cancellation, and digital domain interference cancellation (ADIC) [7]. Practical FD systems have been demonstrated that achieve more than 70 dB [7] or 80 dB [8] reduction of self-interference.

FD can be incorporated in a wireless network in two ways: (i) two-node mode, where two nodes transmit to each other simultaneously, and (ii) three-node mode, where a node (e.g., a cellular Base Station (BS)) simultaneously receives from a node and transmits to another node. The three-node mode can be extended to the more general N-node model, where all the nodes either form a path or a cycle, to receive from the upstream node and transmit to the downstream node simultaneously. FD brings about new challenges to the design of power control algorithms. In a traditional Half-Duplex (HD) network, if a node increases its power, the Signal-to-Interference-Plus-Noise Ratio (SINR) at its target receiver can be improved, but with larger interference to other receivers. In an FD network, an increase in power causes not only larger interference to other receivers, but also larger residual self-interference to the node itself, which may even degrade its own SINR. To fully harvest the high potential of FD wireless networks, the power control problem should be carefully addressed with effective developed algorithms.

In this paper, we first consider an FD wireless network consisting of multiple node pairs, where the two nodes in each pair transmit to each other (i.e., the two-node mode). We analyze the basic case with a single pair of nodes [9]. Taking advantage of the structure of the formulated optimal power control problem, we show that the optimal solution should be at the vertex of the feasible region. Furthermore, we consider the case of multiple node pairs in the FD network. Based on a high SINR approximation, we transform the optimal power control problem

☆ This paper was presented in part at IEEE WCNC 2015, New Orleans, LA, USA, Mar. 2015 [1]. This work is supported in part by the US National Science Foundation under Grants CNS-1247955, and by the Wireless Engineering Research and Education Center (WEREC) at Auburn University, Auburn, AL, USA.
* Corresponding author.
E-mail addresses: yzw0049@tigermail.auburn.edu (Y. Wang), smao@ieee.org (S. Mao).
Peer review under responsibility of Chongqing University of Posts and Telecommunication.

http://dx.doi.org/10.1016/j.dcan.2016.10.004
Received 3 October 2016; Accepted 31 October 2016
Available online 02 November 2016

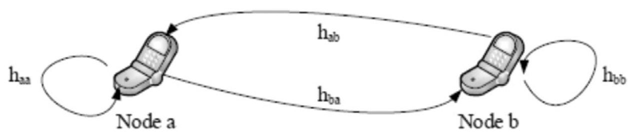

Fig. 1. An FD link consisting of a pair of FD nodes.

into a convex problem in the high SINR region. We develop a Dual Decomposition based distributed algorithm to find the optimal solution to the transformed problem [10]. We then consider the case of general SINR values and drop the high SINR assumption. Incorporating an iterative approximation method for the logarithm functions [12], we are able to obtain a convex transformation of the original power control problem and develop a distributed algorithm.

Finally, we extend our work from the two-node mode to the general FD network scenario, where some of the nodes may be receiving data from one node, while transmitting to another node. We show that the general network graph can be decomposed into isolated nodes, paths, and cycles, for which the distributed power control algorithm still applies to find near optimal power assignments. The proposed algorithms are validated with simulations, where fast convergence and large gain over the traditional HD system are demonstrated.

The remainder of this paper is organized as follows. The system model and preliminaries are introduced in Section 2. We investigate the case of a single pair of FD nodes in Section 3 and a network of FD node pairs in Section 4. We next address the case of a general FD network in Section 5. Simulation results are presented in Section 6. Section 7 reviews related work and Section 8 concludes this paper.

2. System model and preliminaries

We present the channel and propagation model in this section. We then derive the total capacity for a single pair of FD nodes and for an FD network with multiple pairs of FD nodes.

2.1. Channel and propagation models

Consider an FD wireless network that only consists of two transceivers, denoted as nodes a and b, respectively. The FD link is shown in Fig. 1. The received signals at the two transceivers are

$$\begin{cases} y_a = \sqrt{P_b}\,h_{ba}x_b + \sqrt{P_a}\,h_{aa}x_a + n_a \\ y_b = \sqrt{P_a}\,h_{ab}x_a + \sqrt{P_b}\,h_{bb}x_b + n_b \end{cases} \tag{1}$$

where x_a and x_b are the normalized, transmitted signals from node a and b, respectively; P_a and P_b are the corresponding transmitting powers; h_{ab} and h_{ba} are the channel gains from node a to b and from node b to a, respectively; h_{aa} and h_{bb} are the self-interference channel gain at node a and b, respectively; and n_a and n_b are the thermal noises.

According to the channel estimation model in [13], the maximum likelihood channel estimation is modeled as

$$h = \hat{h} + \sqrt{e}\,\tilde{h} \tag{2}$$

where $\hat{h}$ is the estimated channel; $\sqrt{e}\,\tilde{h}$ is the estimation error that is uncorrelated with the real channel h; and $\tilde{h}$ is i.i.d. Gaussian with a zero mean and unit variance. In (2), $\sqrt{e}$ is an indicator that shows how accurate the estimated channel is.

2.2. Propagation-domain interference suppression

Self-interference cancellation is the enabler of FD systems. Among many techniques, propagation domain interference suppression (PDIS) dramatically reduces the self-interference [14]. Applying PDIS, the self-interference terms, e.g., $\sqrt{P_a}\,h_{aa}x_a$, in the received signals (1) is reduced to a fraction, as $\sqrt{\kappa P_a}\,h_{aa}x_a$.

Considering both PDIS and channel estimation, the received signals in (1) can be written as [9]

$$\begin{cases} y_a = \sqrt{P_b}\,\hat{h}_{ba}x_b + \sqrt{\kappa P_a}\,(\hat{h}_{aa} + \sqrt{e_{aa}}\,\tilde{h}_{aa})x_a + n_a \\ y_b = \sqrt{P_a}\,\hat{h}_{ab}x_a + \sqrt{\kappa P_b}\,(\hat{h}_{bb} + \sqrt{e_{bb}}\,\tilde{h}_{bb})x_b + n_b \end{cases} \tag{3}$$

2.3. Analog and digital interference cancellation

In addition to PDIS, analog and digital interference cancellation (ADIC) can cancel more known self-interference. For example, in the first equation in (3), the first term $\sqrt{P_b}\,\hat{h}_{ba}x_b$ is the expected received signal, and the rest of the terms are treated as interference and noise. However, $\sqrt{\kappa P_a}\,\hat{h}_{aa}$ is already known by node a, since the estimated self-interference channel and PDIS of this channel are both known at the node. Therefore, this part of interference is eliminated with ADIC, and the remaining interference plus noise at node a is $\sqrt{\kappa P_b e_{aa}}\,\tilde{h}_{aa}x_a + n_a$.

Denoting $\hat{h}^2$ as $\hat{G}$, the received signal power is $P_b\hat{G}_{ba}$, the remaining interference power after interference cancellation is $\kappa P_a e_{aa}$, and the noise power is N_a. Since both κ and e_{aa} are related to self-interference cancellation, we define a new parameter $\chi = \kappa e_{aa}$ as the *self-interference cancellation coefficient*. The SINRs for FD transceivers a and b are written as

$$SINR_a = \frac{P_b\hat{G}_{ba}}{\chi P_a + N_a} \tag{4}$$

$$SINR_b = \frac{P_a\hat{G}_{ab}}{\chi P_b + N_b} \tag{5}$$

We adopt the Shannon formula $C = B\log_2(1 + \text{SINR})$ to approximate the capacity of a channel with bandwidth B. For brevity, we set B=1 for all the transmitters (i.e., we focus on the spectral efficiency since the channels have identical bandwidths). The total capacity for the pair of FD nodes, C_{ab}, is written as

$$C_{ab} = \log\left(1 + \frac{P_b\hat{G}_{ba}}{\chi P_a + N_a}\right) + \log\left(1 + \frac{P_a\hat{G}_{ab}}{\chi P_b + N_b}\right) \tag{6}$$

Now consider an FD network with M pairs of FD nodes, denoted by $\{\{a_j, b_j\}, j = 1, 2, \ldots, M\}$. The sum rate of the entire network, denoted as C_{total}, is written as

$$\begin{aligned} C_{total} = \sum_{j=1}^{M} C_{a_jb_j} = \sum_{j=1}^{M}\Bigg[&\log\left(1 + \frac{\hat{G}_{b_ja_j}P_{b_j}}{\chi P_{a_j} + \sum_{l\neq j}\hat{G}_{a_la_j}P_{a_l} + \sum_{l\neq j}\hat{G}_{b_la_j}P_{b_l} + N_{a_j}}\right) \\ &+\log\left(1 + \frac{\hat{G}_{a_jb_j}P_{a_j}}{\chi P_{b_j} + \sum_{l\neq j}\hat{G}_{a_lb_j}P_{a_l} + \sum_{l\neq j}\hat{G}_{b_lb_j}P_{b_l} + N_{b_j}}\right)\Bigg] \end{aligned} \tag{7}$$

3. Optimal power control for a pair of FD nodes

We first consider the basic case of a pair of FD nodes, i.e., M=1. The idea is to adjust the transmition powers P_a and P_b so as to maximize the total capacity of the FD link. The sum rate of the pair, C_{ab}, is given in (6). The power control problem for nodes a and b is

$$\max_{\{P_a, P_b\}} \quad C_{ab} \tag{8}$$

$$\text{s. t.} \quad 0 \le P_a \le P_{max} \tag{9}$$

$$0 \le P_b \le P_{max} \tag{10}$$

where (9) and (10) are peak power constraints. We have the following theorem for the power control problem of a single FD pair.

Theorem 1. *In the optimal solution to Problem (8), at least one node transmits at its maximum power P_{max}.*

Proof. Defining $Z = \left(1 + \frac{P_b \widehat{G}_{ba}}{\chi P_a + N_a}\right)\left(1 + \frac{P_a \widehat{G}_{ab}}{\chi P_b + N_b}\right)$, then we have $C_{ab} = \log Z$ and $Z > 0$. Consider a weighted sum of the partial derivatives of C_{ab} with respect to P_a and P_b; the weights are $1/P_b$ and $1/P_a$, respectively. We have

$$\frac{\partial C_{ab}}{\partial P_a}\cdot\frac{1}{P_b} + \frac{\partial C_{ab}}{\partial P_b}\cdot\frac{1}{P_a} = \frac{\widehat{G}_{ba}\widehat{G}_{ab}\chi(2N_aN_b + N_aP_b\chi + N_bP_a\chi)}{Z(\chi P_a + N_a)^2(\chi P_b + N_b)^2} + \frac{\widehat{G}_{ab}N_b}{Z(\chi P_b + N_b)^2 P_b} + \frac{\widehat{G}_{ba}N_a}{Z(\chi P_a + N_a)^2 P_a} > 0 \tag{11}$$

Therefore, the two partial derivatives cannot be both non-positive; we have either $\partial C_{ab}/\partial P_a > 0$ or $\partial C_{ab}/\partial P_b > 0$ (or both) for any power allocation in the feasible region defined in (9) and (10).

Consequently, we can always increase C_{ab} by increasing the power for the node with a positive partial derivative, until finally hitting the boundary of the feasible region. Thus the optimal solution will always be on the boundary of the feasible region, i.e., it will be either (P_a, P_{max}), (P_{max}, P_b), or (P_{max}, P_{max}).□

Based on this observation, the algorithm for computing the optimal power allocation for the FD pair is presented in Algorithm 1. The algorithm basically searches for the optimal solution on the boundary of the feasible region.

Algorithm 1. Optimal Power Control Algorithm for a Single FD Pair.

1 Solve $\left.\frac{\partial C_{ab}}{\partial P_a}\right|_{P_b = P_{max}} = 0$ for P_a;
2 Solve $\left.\frac{\partial C_{ab}}{\partial P_b}\right|_{P_a = P_{max}} = 0$ for P_b;
3 Substitute (P_a, P_{max}) into(6) to get $C_{ab}(1)$;
4 Substitute (P_{max}, P_b) into(6) to get $C_{ab}(2)$;
5 **if** $C_{ab}(1) \geq C_{ab}(2)$ **then**
6 Output optimal power allocation $(P_a^*, P_b^*) = (P_a, P_{max})$;
7 **else**
8 Output optimal power allocation $(P_a^*, P_b^*) = (P_{max}, P_b)$;
9 **end**

In the case of a single pair of FD nodes, increasing the power of one node, say node a, has both positive and negative effects on the sum rate: the SINR for node b will be larger since the received signal will be stronger; but the SINR for node a itself will be smaller, since the self-interference will also go up. Furthermore, at least one of the nodes should transmit at the maximum power according to Theorem 1. In the case of power allocation for a network of FD pairs (i.e., the case when $M > 1$), similar observations can be made, as will be shown in Section 4.

4. Power control for multiple FD node pairs

We next consider the optimal power allocation problem for the case of $M > 1$ pairs of FD nodes. Within each pair, the two FD nodes transmit simultaneously to each other. The challenge is that the power control problem is not convex in the feasible region, and thus cannot be solved by a convex optimization technique directly. We show how to apply two approximation methods to transform the network-wide power control problem into a convex problem.

4.1. High SINR approximation and convexity

In the high SINR region where SINR$\gg$1, we have log(1+SINR) $\approx$ log(SINR). The capacity of an FD link for a given power allocation vector $\mathbf{P}$ can thus be approximated as

$$C_{a_jb_j}^{(1)}(\mathbf{P}) = \log\left(\frac{\widehat{G}_{b_ja_j}P_{b_j}}{\chi P_{a_j} + \sum_{l\neq j}\widehat{G}_{a_la_j}P_{a_l} + \sum_{l\neq j}\widehat{G}_{b_la_j}P_{b_l} + N_{a_j}}\right) + \log\left(\frac{\widehat{G}_{a_jb_j}P_{a_j}}{\chi P_{b_j} + \sum_{l\neq j}\widehat{G}_{a_lb_j}P_{a_l} + \sum_{l\neq j}\widehat{G}_{b_lb_j}P_{b_l} + N_{b_j}}\right) \tag{12}$$

The sum rate of the FD network is approximated as

$$C_{total}^{(1)}(\mathbf{P}) = \sum_{j=1}^{M} C_{a_jb_j}^{(1)}(\mathbf{P}) = \sum_{j=1}^{M}\Bigg[\log\widehat{G}_{a_jb_j} + \log\widehat{G}_{b_ja_j} + \log P_{a_j} + \log P_{b_j} - \log\left(\chi P_{a_j} + \sum_{l\neq j}\widehat{G}_{a_la_j}P_{a_l} + \sum_{l\neq j}\widehat{G}_{b_la_j}P_{b_l} + N_{a_j}\right) - \log\left(\chi P_{b_j} + \sum_{l\neq j}\widehat{G}_{a_lb_j}P_{a_l} + \sum_{l\neq j}\widehat{G}_{b_lb_j}P_{b_l} + N_{b_j}\right)\Bigg] \tag{13}$$

The power control problem for the network of M FD node pairs is formulated as

$$\max_{\{\mathbf{P}\}} \quad C_{total}^{(1)}(\mathbf{P}) \tag{14}$$

$$\text{s. t.} \quad 0 \leq P_{a_j} \leq P_{max}, \quad \text{for all } j \tag{15}$$

$$0 \leq P_{b_j} \leq P_{max}, \quad \text{for all } j \tag{16}$$

where (15) and (16) are the peak power constraints. We next show the problem is convex in the high SINR region.

Theorem 2. *Problem (14) is a convex optimization problem.*

Proof. Define $\widetilde{P}_{x_j} = \log P_{x_j}$, which means $P_{x_j} = e^{\widetilde{P}_{x_j}}$, for all $x \in \{a, b\}$, $j \in \{1, 2, \ldots, M\}$. Consider the problem with variables $\widetilde{\mathbf{P}} = [\widetilde{P}_{a_1}, \widetilde{P}_{b_1}, \ldots, \widetilde{P}_{a_M}, \widetilde{P}_{b_M}]$. Taking the partial derivative of $C_{total}^{(1)}(\widetilde{\mathbf{P}})$ with respect to $\widetilde{P}_{a_j}$, we have that

$$\nabla_{a_j}C_{total}^{(1)}(\widetilde{\mathbf{P}}) = 1 - \sum_{k\neq j}\left(\frac{s_{a_ja_k}}{\sum_l(s_{a_la_k} + s_{b_la_k}) + N_{a_k}} + \frac{s_{a_jb_k}}{\sum_l(s_{a_lb_k} + s_{b_lb_k}) + N_{b_k}}\right)$$

where $s_{a_ja_j} = \chi e^{\widetilde{P}_{a_j}}$, $s_{a_jb_j} = 0$, and $s_{a_jb_l} = \widehat{G}_{a_jb_l}e^{\widetilde{P}_{a_j}}$.

Taking the derivative again for each nonlinear term

$$-\log\left(\chi P_{a_j} + \sum_{l\neq j}\widehat{G}_{a_la_j}P_{a_l} + \sum_{l\neq j}\widehat{G}_{b_la_j}P_{b_l} + N_{a_j}\right)$$

the Hessian is

$$\mathbf{H}^{a_j} = \mathbf{s}_{a_j}^T\mathbf{s}_{a_j} - \text{diag}(\mathbf{s}_{a_j})$$

where $\mathbf{s}_{a_j} = [s_{a_1a_j}, \ldots, s_{b_Ma_j}]/(\sum_k s_{ka_j} + N_{a_j})$. The overall Hessian is $\sum_l \mathbf{s}_l^T\mathbf{s}_l - \text{diag}(\mathbf{s}_l)$, where k and l represent either a_j and b_j. For a non-zero row vector $\mathbf{t}$, we have

$$\mathbf{t}\mathbf{H}\mathbf{t}^T = \sum_l\left(\sum_m\frac{t_ms_{ml}}{\sum_k s_{kl} + N_l}\right)^2 - \sum_l\sum_m\frac{t_m^2s_{ml}}{\sum_k s_{kl} + N_l} = \sum_l\frac{\sum_m(t_ms_{ml})^2 - \sum_m t_m^2s_{ml}(\sum_k s_{kl} + N_l)}{(\sum_k s_{kl} + N_l)^2} < \sum_l\frac{\sum_m(t_ms_{ml})^2 - \sum_m t_m^2s_{ml}(\sum_m s_{ml})}{(\sum_k s_{kl} + N_l)^2} \tag{17}$$

The inequality (17) is due to the omission of some negative terms, i.e.,

$-\sum_l \sum_m t_m^2 s_{ml} N_l / (\sum_k s_{kl} + N_l)^2$. For each numerator, letting $\phi_m = t_m \sqrt{s_{ml}}$ and $\theta_m = \sqrt{s_{ml}}$, we have $\sum_m (t_m s_{ml})^2 - \sum_m t_m^2 s_{ml} (\sum_m s_{ml}) \le 0$, for all l, according to the Cauchy-Schwarz Inequality (i.e., $(\boldsymbol{\phi}^T \boldsymbol{\theta})^2 \le (\boldsymbol{\phi}^T \boldsymbol{\phi})(\boldsymbol{\theta}^T \boldsymbol{\theta})$). Thus $\mathbf{tHt}^T < 0$, and $C_{total}^{(1)}(\widetilde{\mathbf{P}})$ is concave.

Consider the solution space of $\mathbf{P}$, it is easy to verify that $\nabla_{aj} C_{total}^{(1)}(\mathbf{P}) = \frac{1}{P_{aj}} \nabla_{aj} C_{total}^{(1)}(\widetilde{\mathbf{P}})$. The transformation from $\mathbf{P}$ to $\widetilde{\mathbf{P}}$ only scales the gradient, but does not affect the concavity property. Thus $C_{total}^{(1)}(\mathbf{P})$ is also concave. With linear constraints (15) and (16), problem (14) is a convex optimization problem. □

4.2. Decomposition and distributed algorithm

We next apply the *Dual Decomposition* technique to develop a distributed power control algorithm for the FD network [10,11]. Rewrite the sum rate approximation (13) as

$$C_{total}^{(1)}(\mathbf{P}) = \sum_{j=1}^{M} C_{a_j b_j}^{(1)}(\mathbf{P}) = \sum_{j=1}^{M} \left[\log\left(\frac{\widehat{G}_{a_j b_j} P_{a_j}}{\chi P_{b_j} + m_{b_j}} \right) + \log\left(\frac{\widehat{G}_{b_j a_j} P_{b_j}}{\chi P_{a_j} + m_{a_j}} \right) \right] \tag{18}$$

where

$$\begin{cases} m_{a_j} = \sum_{l \ne j} \widehat{G}_{a_l a_j} P_{a_l} + \sum_{l \ne j} \widehat{G}_{b_l a_j} P_{b_l} + N_{a_j} \\ m_{b_j} = \sum_{l \ne j} \widehat{G}_{a_l b_j} P_{a_l} + \sum_{l \ne j} \widehat{G}_{b_l b_j} P_{b_l} + N_{b_j} \end{cases} \tag{19}$$

are the received signals for idle nodes a_j and b_j, i.e., the interference plus noise at nodes a_j and b_j from other nodes, respectively.

Problem (14) is rewritten as maximizing (18) subject to constraints (15), (16), and (19). Define the Lagrange multipliers $\boldsymbol{\mu}$ and consider the *Lagrangian* only including the coupled constraints. We have

$$\begin{aligned} \mathcal{L}^{(1)}(\mathbf{P}, \boldsymbol{\mu}) &= C_{total}^{(1)}(\mathbf{P}) \\ &\quad + \sum_{j=1}^{M} \left[\mu_{a_j} \left(m_{a_j} - \sum_{l \ne j} \widehat{G}_{a_l a_j} P_{a_l} - \sum_{l \ne j} \widehat{G}_{b_l a_j} P_{b_l} - N_{a_j} \right) \right. \\ &\quad \left. + \mu_{b_j} \left(m_{b_j} - \sum_{l \ne j} \widehat{G}_{a_l b_j} P_{a_l} - \sum_{l \ne j} \widehat{G}_{b_l b_j} P_{b_l} - N_{b_j} \right) \right] \\ &= \sum_{j=1}^{M} \left(C_{a_j b_j}^{(1)} - \nu_{a_j} P_{a_j} - \nu_{b_j} P_{b_j} \right) + \sum_{j=1}^{M} (\mu_{a_j} m_{a_j} + \mu_{b_j} m_{b_j}) \end{aligned}$$

where $C_{a_j b_j}^{(1)}$ is the capacity for FD node pair $\{a_j, b_j\}$; $\nu_{aj} = \sum_{l=1}^{M} \mu_{a_l} \widehat{G}_{a_j a_l} + \sum_{l=1}^{M} \mu_{b_l} \widehat{G}_{a_j b_l}$; and $\nu_{b_j} = \sum_{l=1}^{M} \mu_{a_l} \widehat{G}_{b_j a_l} + \sum_{l=1}^{M} \mu_{b_l} \widehat{G}_{b_j b_l}$.

The subproblem for each pair of nodes $\{a_j, b_j\}$ is

$$\max_{\{P_{a_j}, P_{b_j}\}} \quad C_j^{(1)}(P_{a_j}, P_{b_j}) = C_{a_j b_j}^{(1)}(P_{a_j}, P_{b_j}) - \nu_{a_j} P_{a_j} - \nu_{b_j} P_{b_j} \tag{20}$$

$$\text{s. t.} \quad 0 \le P_{a_j} \le P_{max} \tag{21}$$

$$0 \le P_{b_j} \le P_{max} \tag{22}$$

The optimal solution $\{P_{a_j}^*, P_{b_j}^*\}$ can be solved by local *Karush-Kuhn-Tucher* (KKT) Conditions or using the subgradient method.

The master problem is written as

$$\min_{\boldsymbol{\mu}} \quad C_{total}^{(1)}(\boldsymbol{\mu}) = \sum_{j=1}^{M} C_j^{(1)}(\boldsymbol{\mu}) + \sum_{j=1}^{M} (\mu_{a_j} m_{a_j} + \mu_{b_j} m_{b_j}) \tag{23}$$

$$\text{s. t. } \boldsymbol{\mu} \ge \mathbf{0} \tag{24}$$

The gradient method is used to solve the master problem by using a centralized controller or by flooding the power allocation information to all other nodes as in [11].

The distributed power control algorithm for the network of FD node pairs is presented in Algorithm 2.

Algorithm 2. Distributed Optimal Algorithm for M Pair of FD Nodes in the High SINR Region.

Initialize μ_{a_j} and μ_{b_j} to some non-negative values, for all j;
repeat
  Each FD pair receives power updates from other nodes;
  Each FD pair computes $m_{a_j}(t)$ and $m_{b_j}(t)$, and solves (23) to update μ_{a_j}, μ_{b_j}, ν_{a_j}, and ν_{b_j};
  Each FD pair solves (20) for $\{P_{a_j}^*, P_{b_j}^*\}$;
  Each FD pair distributes $\{P_{a_j}^*, P_{b_j}^*\}$ to the entire network;
until *convergence*;

4.3. Approximation for general SINR values

Note that Algorithm 2 is based on the high SINR assumption, which may not be true in a general FD network environment, although we can always exclude low SINR transceivers to enforce this assumption. In this section, we present an alternative approach to relax the high SINR assumption, to obtain a more general approximation for the power allocation problem.

Following the approach in [12], the tightest lower bound for $\log(1+x)$ is $\alpha \log x + \beta$, i.e.,

$$\log(1+x) \ge \alpha \log x + \beta, \tag{25}$$

which intersects $\log(1+x)$ at x_0 when the coefficient α and β are chosen as follows.

$$\begin{cases} \alpha = \dfrac{x_0}{1+x_0} \\ \beta = \log(1+x_0) - \dfrac{x_0}{1+x_0} \log x_0 \end{cases} \tag{26}$$

The lower-bounding approximation to the log-function is illustrated in Fig. 2. It can be seen that the approximation curve is always below the log-function curve, and the two curves intersect at x_0.

Let $\mathbf{P} = \{P_1, P_2, \ldots, P_M\}$, $\boldsymbol{\alpha} = \{\alpha_1, \alpha_2, \ldots, \alpha_M\}$, and $\boldsymbol{\beta} = \{\beta_1, \beta_2, \ldots, \beta_M\}$. We approximate the network-wide sum rate as

$$\begin{aligned} C_{total}^{(2)}(\mathbf{P}, \boldsymbol{\alpha}, \boldsymbol{\beta}) &= \sum_{j=1}^{M} C_{a_j b_j}^{(2)}(\mathbf{P}, \boldsymbol{\alpha}, \boldsymbol{\beta}) \\ &= \sum_{j=1}^{M} \left[\alpha_{a_j} \log\left(\frac{\widehat{G}_{b_j a_j} P_{b_j}}{\chi P_{a_j} + m_{a_j}} \right) + \beta_{a_j} \right. \\ &\quad \left. + \alpha_{b_j} \log\left(\frac{\widehat{G}_{a_j b_j} P_{a_j}}{\chi P_{b_j} + m_{b_j}} \right) + \beta_{b_j} \right] \end{aligned} \tag{27}$$

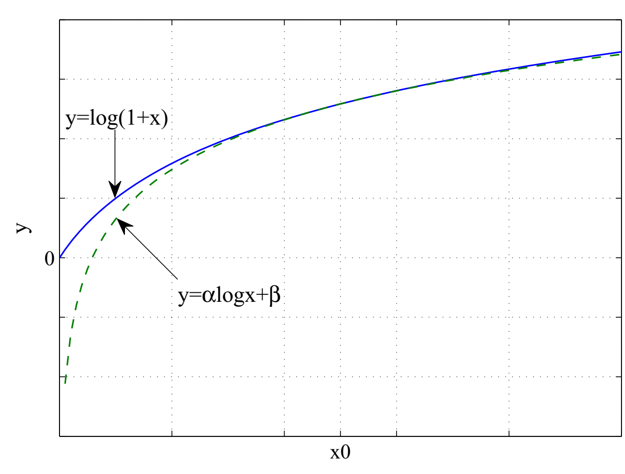

Fig. 2. A lower-bounding approximation to the log-function.

The power control problem for M FD node pairs becomes

$$\max_{\mathbf{P}} \quad C_{total}^{(2)}(\mathbf{P}, \boldsymbol{\alpha}, \boldsymbol{\beta})$$
$$\text{s. t. constraints (15), (16), and (19).} \tag{28}$$

It can be shown that $C_{total}^{(2)}(\mathbf{P})$ is also concave, following a similar approach as that in Section 4.1. This is because the non-negative and constant scalars $\boldsymbol{\alpha}$ and $\boldsymbol{\beta}$ do not change the concavity property. Hence $C_{total}^{(2)}(\mathbf{P})$ is concave for non-negative $\boldsymbol{\alpha}$ and $\boldsymbol{\beta}$; the method of Dual Decomposition is applied to find the optimal solution for a given $\boldsymbol{\alpha}$ and $\boldsymbol{\beta}$.

To further improve the competitiveness of the solution, we iteratively update $\boldsymbol{\alpha}$ and $\boldsymbol{\beta}$ in each step τ as follows, until the optimal solution to the original problem is achieved.

$$\begin{cases} x_{a_j}(\tau) = \dfrac{\widehat{G}_{b_ja_j}P_{b_j}^{*}(\tau)}{\chi P_{a_j}^{*}(\tau) + m_{a_j}(\tau)} \\ \alpha_{a_j}(\tau) = \dfrac{x_{a_j}(\tau)}{1 + x_{a_j}(\tau)} \\ \beta_{a_j}(\tau) = \log(1 + x_{a_j}(\tau)) - \dfrac{x_{a_j}(\tau)}{1 + x_{a_j}(\tau)}\log(x_{a_j}(\tau)) \end{cases} \tag{29}$$

$$\begin{cases} x_{b_j}(\tau) = \dfrac{\widehat{G}_{a_jb_j}P_{a_j}^{*}(\tau)}{\chi P_{b_j}^{*}(\tau) + m_{b_j}(\tau)} \\ \alpha_{b_j}(\tau) = \dfrac{x_{b_j}(\tau)}{1 + x_{ab_j}(\tau)} \\ \beta_{b_j}(\tau) = \log(1 + x_{b_j}(\tau)) - \dfrac{x_{b_j}(\tau)}{1 + x_{b_j}(\tau)}\log(x_{b_j}(\tau)) \end{cases} \tag{30}$$

Algorithm 3. Distributed Optimal Algorithm for M Pair of FD Nodes in the Case of General SINR Values.

Set $\tau = 0$, and $\boldsymbol{\alpha}(0) = \mathbf{1}$, $\boldsymbol{\beta}(0) = \mathbf{0}$;
repeat
    Initialize λ_{a_j} and λ_{b_j} to some non−negative values, and set $m_{a_j} = 0$ and $m_{b_j} = 0$, for all j;
    repeat
        Each FD pair receives updated powers from other nodes;
        Each FD pair computes m_{a_j} and m_{b_j},
        and solves the master problem to update μ_{a_j}, μ_{b_j} and ν_{a_j}, ν_{b_j};
        Each FD pair solves the subproblem for $\{P_{a_j}^{*}, P_{b_j}^{*}\}$;
        Each FD pair distributes $\{P_{a_j}^{*}, P_{b_j}^{*}\}$ to the entire network;
    until *convegence*;
    Each FD pair updates $\alpha_{a_j}(\tau)$, $\alpha_{b_j}(\tau)$, $\beta_{a_j}(\tau)$, and $\beta_{b_j}(\tau)$ as in (29) and (30); $\tau \leftarrow \tau + 1$;
until *convegence*;

The distributed power control algorithm for the general network/SINR case is presented in Algorithm 3. Specifically, in each iteration, $m_{a_j}(\tau)$ and $m_{b_j}(\tau)$ can be sensed from the radio environment. We then use them to compute $x_{a_j}(\tau)$ as in (29), using $x_{a_j}(\tau)$ to update $\alpha_{a_j}(\tau)$ and $\beta_{a_j}(\tau)$, and using $x_{b_j}(\tau)$ to update $\alpha_{b_j}(\tau)$ and $\beta_{b_j}(\tau)$. Finally the new power assignment $\mathbf{P}(\tau + 1)$ is derived based on $\boldsymbol{\alpha}(\tau)$ and $\boldsymbol{\beta}(\tau)$.

5. Power control in a general FD network

In Sections 3 and 4, we mainly focus on the two-node FD transmission scenario, where the FD nodes are paired to transmit to and receive from each other. In this section, we consider the more general case of FD networks. We assume a link scheduling algorithm in force, which schedules FD and/or HD transmissions for the FD nodes, based on their traffic demand. As a result, in the graph formed by the nodes and active links, each of the FD nodes will have a node degree of either 0 (if it is not scheduled to transmit or receive), or 1 (if it is a HD transmitter or receiver), or 2 (if it is scheduled to transmit and receive simultaneously).

The snapshot of the FD network with nodes and active links, termed *transmission graph* in this paper, will thus consist of various subgraphs, such as an isolated vertex (no transmissions and thus no need for power control), a path (or, an open walk), and a cycle (or, a closed walk). In the case of a path, the head and tail node of the path operate in HD transmit and receive mode, respectively, while each intermediate node operates in FD mode, receiving from the previous node while transmitting to the next node in the path. In the case of a cycle, each node operates in FD node, receiving from the previous node while transmitting to the next node. When the cycle consists of only two nodes, it reduces to the FD pair case we studied in the previous two sections. Some examples are given in Fig. 3.

In the following, we first examine the problem of power control in the basic three-node cycle case. We then show that a general FD network can be decomposed to basic elements and show how to perform power control in the general FD network.

5.1. Basic three-node FD cycle

Consider the basic scenario of a three-node cycle. In the cycle, node a transmits to node b, while receiving data from node c; node b transmits to node c, while receiving data from node a. The sum rate of the 3 nodes, denoted as C_{abc}, is

$$C_{abc} = \log\left(1 + \frac{P_a\widehat{G}_{ab}}{\chi P_b + P_c\widehat{G}_{cb} + N_b}\right) + \log\left(1 + \frac{P_b\widehat{G}_{bc}}{\chi P_c + P_a\widehat{G}_{ac} + N_c}\right) + \log\left(1 + \frac{P_c\widehat{G}_{ca}}{\chi P_a + P_b\widehat{G}_{ba} + N_a}\right) \tag{31}$$

The optimal power control problem for this three-node network can be formulated as

$$\max_{\{P_a, P_b, P_c\}} \quad C_{abc} \tag{32}$$

$$\text{s. t.} \quad 0 \le P_a \le P_{max} \tag{33}$$

$$0 \le P_b \le P_{max} \tag{34}$$

$$0 \le P_c \le P_{max} \tag{35}$$

Let $\mathbf{P} = \{P_a, P_b, P_c\}$, $\boldsymbol{\alpha} = \{\alpha_a, \alpha_b, \alpha_c\}$, and $\boldsymbol{\beta} = \{\beta_a, \beta_b, \beta_c\}$. Applying the lower bound approximation for logarithm functions (25), we have

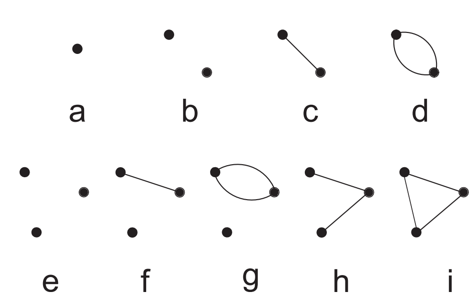

Fig. 3. The basic cases of $N \le 3$.

$$
\begin{aligned}
C_{abc}^{(2)}(\mathbf{P},\boldsymbol{\alpha},\boldsymbol{\beta}) &= \alpha_a \log\left(\frac{\widehat{G}_{ca}P_c}{\chi P_a + P_b\widehat{G}_{ba} + N_a}\right) + \beta_a \\
&\quad + \alpha_b \log\left(\frac{\widehat{G}_{ab}P_a}{\chi P_b + P_c\widehat{G}_{cb} + N_b}\right) + \beta_b \\
&\quad + \alpha_c \log\left(\frac{\widehat{G}_{bc}P_b}{\chi P_c + P_a\widehat{G}_{ac} + N_c}\right) + \beta_c \\
&= \alpha_a \log\widehat{G}_{ca} + \alpha_b\log\widehat{G}_{ab} + \alpha_c\log\widehat{G}_{bc} + \beta_a + \beta_b + \beta_c \\
&\quad + \alpha_a\log P_c + \alpha_b \log P_a + \alpha_c \log P_b \\
&\quad - \alpha_a \log(\chi P_a + P_b\widehat{G}_{ba} + N_a) \\
&\quad - \alpha_b \log(\chi P_b + P_c\widehat{G}_{cb} + N_b) \\
&\quad - \alpha_c \log(\chi P_c + P_a\widehat{G}_{ac} + N_c) \qquad (36)
\end{aligned}
$$

Therefore, the sum rate (31) is transformed into a sum of logarithms, each being a logarithm of a linear combination of P_a, P_b, and P_c. The approximated problem is concave and also solved with Algorithm 3.

The above result is extended to a general FD cycle, as given in the following lemma.

Lemma 1. *Suppose there are N nodes, i.e., x_1, x_2, $\cdots$, and x_N, that form a cycle, where node x_i transmits to node x_{i+1}, for all $1 \le i \le N-1$, and node x_N transmits to node 1. Suppose there are M other nodes, i.e., y_1, y_2, $\cdots$, and y_M outside the cycle, which may cause interference to the nodes in the cycle. Then the sum rate for the N-node cycle is transformed into a sum of logarithms of linear combinations of the transmit powers, i.e., P_{x_1}, P_{x_2}, $\cdots$, P_{x_N}, P_{y_1}, P_{y_2}, $\cdots$, and P_{y_M}.*

Proof. As in the case of the three-node cycle, the sum rate of the N-node cycle is written as (note that $x_{N+1} = x_1$)

$$
C_{cycle} = \sum_{i=1}^{N} \log\left(1+\frac{P_{x_i}\widehat{G}_{x_ix_{i+1}}}{\chi P_{x_{i+1}} + \sum_{j\neq i,i+1} P_{x_j}\widehat{G}_{x_jx_{i+1}} + \sum_{k=1}^{M} P_{y_k}\widehat{G}_{y_kx_{i+1}} + N_{x_{i+1}}}\right)
$$

Applying the lower bound approximation for logarithm functions (25), we have

$$
\begin{aligned}
C_{cycle}^{(2)}(\mathbf{P},\boldsymbol{\alpha},\boldsymbol{\beta}) &= \sum_{i=1}^{N} \alpha_{x_{i+1}}\log\widehat{G}_{x_ix_{i+1}} + \beta_{x_{i+1}} + \alpha_{x_{i+1}}\log P_{x_i} \\
&\quad - \alpha_{x_{i+1}}\log\left(\chi P_{x_{i+1}} + \sum_{j\neq i,i+1} P_{x_j}\widehat{G}_{x_jx_{i+1}} + \sum_{k=1}^{M} P_{y_k}\widehat{G}_{y_kx_{i+1}} + N_{x_{i+1}}\right) \qquad (37)
\end{aligned}
$$

From Lemma 1, the lower capacity bound $C_{cycle}^{(2)}(\mathbf{P},\boldsymbol{\alpha},\boldsymbol{\beta})$ is also concave. Therefore, the power allocation problem for a cycle component of a general FD network is solved with Algorithm 3.

5.2. General FD networks

Finally, we consider the case of a general FD network. As discussed, with the link scheduling mechanism in force, the transmission graph is a graph where each vertex represents a node, and each edge represents an active link between two nodes. Since each node at most transmits to another node and/or receives from the same, or another node, the in-degree (i.e., the number of incoming edges) and the out-degree (i.e., the number of outgoing edges) of each node is at most 1, and the node degree is at most 2. Then we have the following theorem for the general FD network.

Theorem 3. *A directed graph **G** with a maximum node degree of 2, is composed of isolated vertices, paths, and cycles.*

Proof. We prove the theorem by induction with respect to the number of vertices N of the graph $\boldsymbol{G}$. For the base case of $N \le 3$, we simply

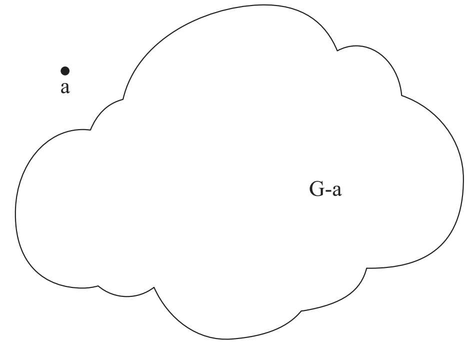

Fig. 4. The degree of vertex a is 0.

enumerate all possible scenarios, as given in Fig. 3. Note that in Figs. 3–8, the links are directional but the directions are omitted for clarity.

The hypothesis assumption is that the theorem holds true for any directional graphs $\boldsymbol{G}_a$ with k or fewer vertices. Now, we show that the theorem also holds true when an additional vertex a is added to the graph, to form a new directional graph $\boldsymbol{G}$ with $k+1$ vertices. Since the degree of vertex a is either 0, 1, and 2, we examine these cases in the following.

- When the deg(a)=0: as shown in Fig. 4, vertex a is an isolated vertex. Since the theorem holds true for $\boldsymbol{G}_a$ with k vertices following the hypothesis assumption, then $\boldsymbol{G}$ only contains isolate vertices, paths, and cycles.
- When the deg(a)=1, vertex a has only one neighbor, termed vertex b in $\boldsymbol{G}_a$. We have the following two cases. If deg(b)=1, as in Fig. 5, then edge ab (or ba) forms a path in $\boldsymbol{G}$. If the deg(b)=2, as in Fig. 6, then vertex b is an endpoint of a path P in $\boldsymbol{G}_a$, and $a \cup P$ forms a longer path in $\boldsymbol{G}$. Following the hypothesis assumption, $\boldsymbol{G}$ only contains isolate vertices, paths, and cycles.
- When the deg(a)=2, vertex a has two neighbors, say, vertices b and c. We have the following three cases. If both vertices b and c have a degree of 1, then nodes a, b, and c form a path in the augmented graph $\boldsymbol{G}$. If both vertices b and c have a degree of 2, then we have two cases. First, vertices b and c are the endpoints of two different paths in graph $\boldsymbol{G}_a$. Then vertex a connects the two paths to form a longer path, a shown in Fig. 7. Second, vertices b and c are the endpoints of the same path in $\boldsymbol{G}_a$. Then vertex a connects vertices b and c to form a new cycle in graph $\boldsymbol{G}$, as shown in Fig. 8. Following the hypothesis assumption, $\boldsymbol{G}$ only contains isolate vertices, paths, and cycles.

In conclusion, considering the base case and the hypothesis induction, we can claim that for all N, a graph with N vertices and

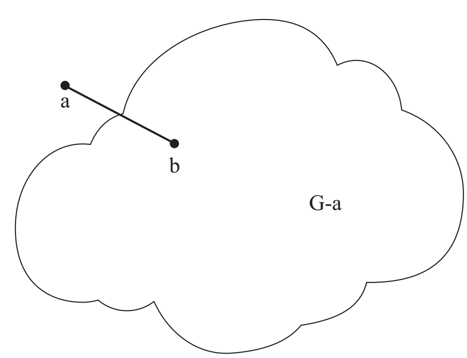

Fig. 5. The degree of vertex a is 1 and its neighbor is an isolated vertex in $\boldsymbol{G}_a$.

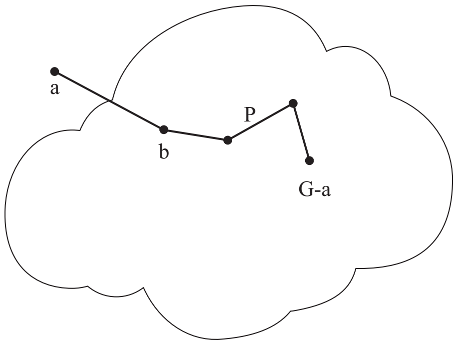

Fig. 6. The degree of vertex a is 1 and its neighbor is the head or tail of a path in $\boldsymbol{G}_a$.

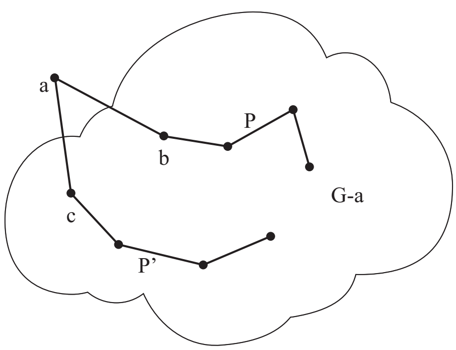

Fig. 7. The degree of vertex a is 2 and its two neighbors are the head or tail of two different paths in $\boldsymbol{G}_a$.

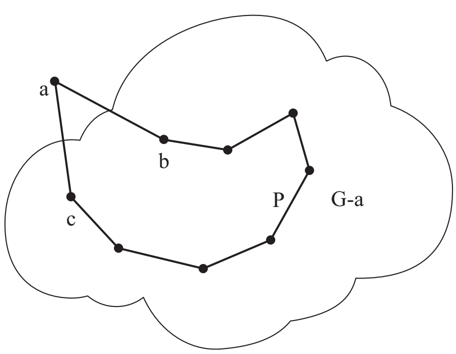

Fig. 8. The degree of vertex a is 2 and its 2 neighbors are the head and tail of the same path in $\boldsymbol{G}_a$.

maximum node degree 2, is composed of isolated vertices, paths, and cycles. □

Theorem 3 shows that a general FD network can be decomposed into isolated nodes, paths, and cycles. From the power control perspective, we have (i) For the isolated nodes, they do not need to communicate with other nodes and their transmission power should be set to 0. (ii) For the nodes that are in cycles, according to Lemma 1, we transform the sum rate into a sum of logarithms of linear combinations of the transmit powers, which can then be solved by a convex optimization solver. (iii) For the nodes that are in paths, a path is a special case of cycle. The tail node does not transmit and its power should be set to 0.

Therefore, for a general FD network, we use Algorithm 4 to solve for the near optimal transmit powers. Note that each node executes the algorithm to compute its transmit power, but they do not need to know the topology of the transmission graph.

Algorithm 4. Distributed Power Control Algorithm for General Full Duplex Networks.

Set $\tau = 0$, and $\boldsymbol{\alpha}(0) = \mathbf{1}$, $\boldsymbol{\beta}(0) = \mathbf{0}$;
repeat
  Initialize $\boldsymbol{\lambda}$ to some non−negative values, and set $\boldsymbol{m} = 0$;
  repeat
    Each FD node receives updated powers from other nodes;
    Each FD node computes m_i
      and solves the master problem to update μ_i and ν_i;
    Each FD node solves the subproblem for P_i^*;
    Each FD nodes distributes P_i^* to the entire network;
  until *convergence*;
  Each FD node updates $\alpha_i(\tau)$ and $\beta_i(\tau)$;
  $\tau \leftarrow \tau + 1$;
until convergence;

6. Simulation results

In this section, we validate the proposed algorithms with simulations. We first examine the case of one pair of FD nodes with unbiased noise. We use an HD network with the same setting as a benchmark; a simplified version of the proposed algorithm is used to find the optimal powers for the HD only network. Note that in the FD network, it is possible that the optimal power for some nodes are zero, indicating that such nodes operate in the HD mode. In the simulations, we assume log-normal block fading channels, with zero mean and 10 dB standard deviation. The path loss exponent is 4. The noise powers are randomly generated around −110 dB W, unless otherwise specified. The results are presented for a time slot within which the channel gains do not vary. The peak power is set to $P_{max} = 5$ mW.

We first demonstrate the impact of the self-interference coefficient χ and noise on FD transmissions in Figs. 9 and 10. In Fig. 9, we plot the normalized throughput as a function of χ. It is seen that, as χ is increased, the normalized throughput of the FD network converges to that of the HD network. Particularly, when χ is less than −45 dB, FD achieves a significant throughput gain over HD; the more effective the self-interference cancellation, the higher the throughput gain.

In Fig. 10, we fix $\chi = -80$ dB and plot the normalized system throughput for increased noise levels. In this simulation, the FD

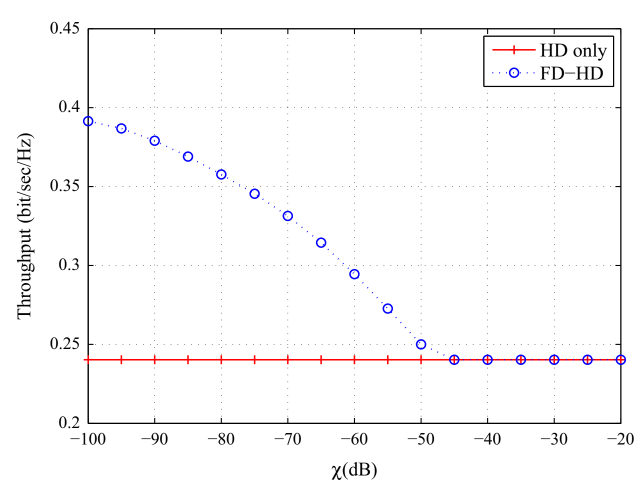

Fig. 9. Optimal throughput of a single pair of FD nodes versus χ.

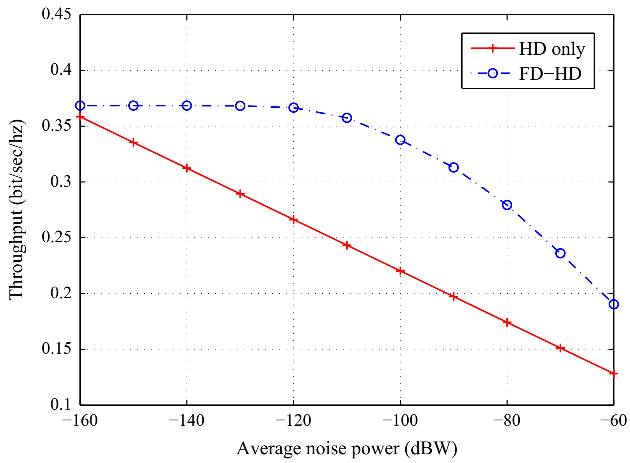

Fig. 10. Optimal throughput of a single pair of FD nodes versus noise level.

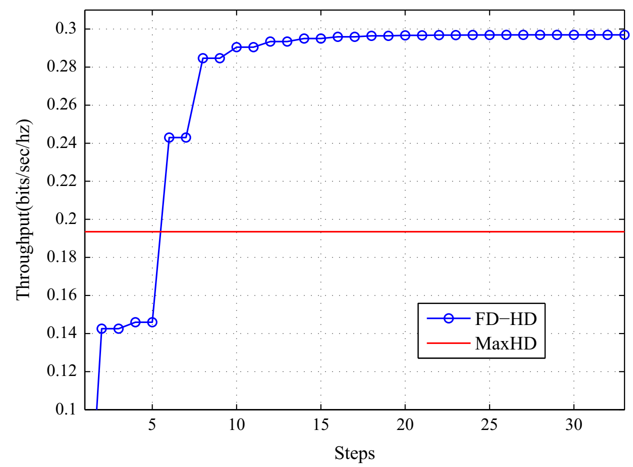

Fig. 12. Convergence of the sum rate of four pairs of FD nodes.

throughput is always higher than that of the HD for the entire range of simulated noise levels. As the noise level is decreased, especially when the average noise power is lower than −120 dB, the FD network throughput approaches that of the HD network. This is because when the noise is extremely low, if one of the nodes, say node b, has $P_b \to 0$, the denominator of SINR_b (see (4)) will be reduced close to zero. The throughput of node b will be dramatically increased, which dominates the reduction in the throughput of node a. Thus the pair will work in HD mode.

Next, we demonstrate the performance of the proposed algorithms for a bidirectional FD network of M=4 node pairs. The general approximation algorithm shown in Algorithm 3 is used to obtain the results shown in Figs. 11 and 13. The convergence of the eight transmition powers are plotted in Fig. 11. With the proposed algorithm, all the transmition powers converge to the optimal power allocation after several iterations. After convergence, node 2 transmits at the maximum power P_{max}, nodes 3, 4, 7, and 8 are not allowed to transmit (with transmit power zero), and nodes 1, 5, and 6 assume some transmition power lower than P_{max}. This is consistent with the single pair of nodes case in Theorem 1 (i.e., at least one node transmits at the peak power). Among the four node pairs, two of them operate in FD mode (1–2 and 5–6), while two of them are turned off (3–4 and 7–8), in order to achieve a larger sum rate. As the channels vary over time slots, the node pairs with power zero in this time slot will get their turn to transmit in future time slots.

The convergence of the sum rate is presented in Fig. 12. We find that the sum rate also converges after several iterations. With Algorithm 3, the sum rate is always non-decreasing across the

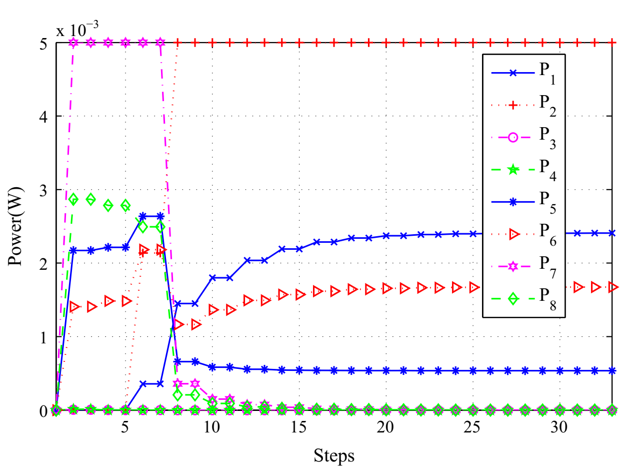

Fig. 11. Convergence performance of the proposed algorithm for four pairs of FD nodes.

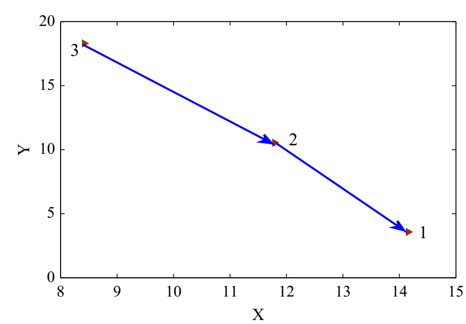

Fig. 13. Basic 3-node FD model: scenario 1.

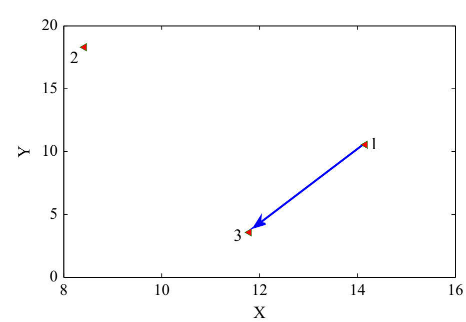

Fig. 14. Basic 3-node model: scenario 2.

iterations. The optimal sum rate of the FD network is about 1.6 times of that of the HD network, demonstrating the benefits of FD transmissions and distributed power control.

In Figs. 13 and 14, we examine the basic three-node FD model assuming all the nodes need to transmit. The general algorithm shown in Algorithm 4 is used to obtain the transmition powers. From the output of our algorithm, the transmition powers for node 1, 2, and 3 in Fig. 13 are 0 mW, 5 mW, and 5 mW, respectively. The transmition powers for node 1, 2, and 3 in Fig. 14 are 5 mW, 0 mW and 0 mW, respectively. These results imply that the FD mode may not always be beneficial. In Fig. 13, node 3 has less interference to node 1, so that the near optimal throughput is achieved when both nodes 2 and 3 nodes transmit simultaneously. However, in the scenario in Fig. 14, only node 1 transmits in the near optimal scenario.

Finally, we simulate a general scenario as shown in Fig. 15, where four FD links transmit simultaneous on the same channel. With each three-node FD link, the three nodes form a path, while the node in the middle operates in FD mode. The self-interference cancellation coefficient is $\chi = -80$ dB. This is like a small cell/femtocell deployment scenario where the BS is in the FD mode, the user equipment is in HD mode,

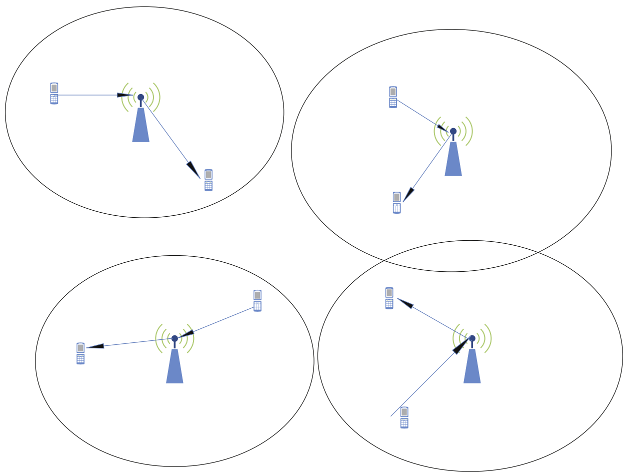

Fig. 15. General scenario of four three-node FD links.

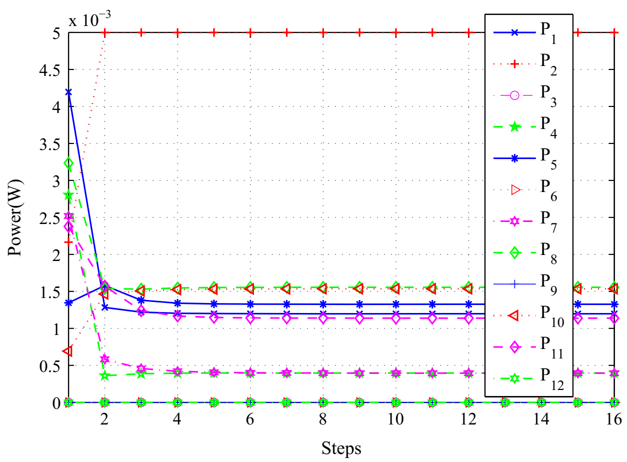

Fig. 16. Convergence performance of the proposed algorithm for the general FD network.

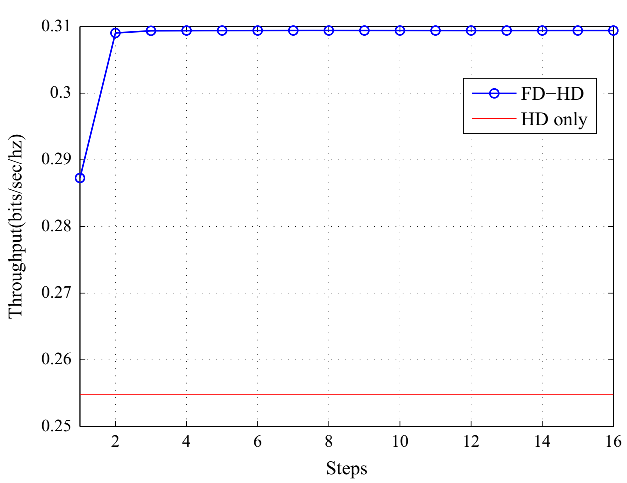

Fig. 17. Convergence performance of the proposed algorithm for the general FD network.

and the four small cells share the same channel. The convergence of the transmit powers are presented in Fig. 16, and the convergence of the network-wide throughput is shown in Fig. 17, where fast convergence is observed. The FD enabled network achieves a 1.2 times higher throughput than the corresponding HD network in this case.

7. Related work

We briefly review related work on FD in this section. FD has become a hot research area in recent years [14–16]. There have been several seminal works on both the theoretic aspect (such as deriving the capacity region [3]) and practical design of FD wireless networks [4]. A practical design and implementation was reported in [4], including the antenna structure, several kinds of self-interference cancellation techniques, and MAC layer design. The authors showed that up to 73 dB suppression of self-interference for a 10 MHz OFDM signal and at least 45 dB reduction at a 40 MHz channel are achievable. Various self-interference cancellation schemes have been investigated in prior works [5–7], such as PDIS, Analog Self-Interference Cancellation, which reduces the self-signal by the design of distance between transmitting antenna and receiving antenna, and Digital Self-Interference Cancellation [4,7,14,17], which cancels the self-signal by subtracting the transmitted signal from the receiving signal. In [8], the details of self-interference cancellation was reviewed and the paper then focused on antenna design, including the arrangement of the position of transmitting and receiving antennas.

In [9], the authors studied power allocation for a single pair of FD nodes equipped with MIMO. It was assumed that the power for each single antenna at the same node were equal. The two transmition powers for the FD pair were then optimized to achieve the maximum throughput. In [18], we studied power control for an underlay cognitive ratio network with FD transmissions, and developed a centralized scheme with a control-theoretic approach. In [19,20], we investigated the incorporation of FD transmissions in cognitive femtocell networks, and developed a matching based algorithm for joint duplex mode selection, channel allocation, and power control for FD cognitive femtocell networks.

8. Conclusion

In this paper, we developed distributed algorithms for near optimal power control in FD wireless networks. For the case of a single pair of FD nodes, we presented a simple algorithm that computed the optimal powers. For the case of multiple pairs of FD nodes, we first developed a distributed algorithm by applying the high SINR approximation, and then proposed a distributed algorithm based on an iterative approximation method for the logarithm function. For general FD networks, we examined the performance for the basic 3-node mode, and showed that a general FD network can be decomposed into isolated nodes, paths, cycles, for which the power control problem was solved with the proposed distributed algorithm. The proposed algorithms were validated with simulation studies.

References

[1] Y. Wang, S. Mao, Distributed power control in full duplex wireless networks, in: Proceedings IEEE WCNC 2015, New Orleans, LA, Mar. 2015, pp. 1165–1170.
[2] C.U. Saraydar, N.B. Mandayam, D. Goodman, Efficient power control via pricing in wireless data networks, IEEE Trans. Commun. 50 (2) (2002) 291–303.
[3] V.R. Cadambe, S.A. Jafar, Degrees of freedom of wireless networks with relays, feedback, cooperation, and full duplex operation, IEEE Trans. Inf. Theory 55 (5) (2009) 2334–2344.
[4] M. Jain, J.I. Choi, T. Kim, D. Bharadia, S. Seth, K. Srinivasan, P. Sinha, Practical, real-time, full duplex wireless, in: Proceedings ACM MobiCom'11, Las Vegas, NV, Sept. 2011, pp. 301–312.
[5] E. Ahmed, A.M. Eltawil, A. Sabharwal, Rate gain region and design tradeoffs for full-duplex wireless communications, IEEE Trans. Wirel. Commun. 12 (7) (2013) 3556–3565.
[6] B.P. Day, A.R. Margetts, D.R. Bliss, P. Schniter, Full-duplex bidirectional MIMO: achievable rates under limited dynamic range, IEEE Trans. Signal Process. 60 (July (7)) (2012) 3702–3713.
[7] M. Duarte, A. Sabharwal, Full-duplex wireless communications using off-the-shelf radios: Feasibility and first results, in: Proceedings IEEE ASILOMAR'10, Pacific Grove, CA, Nov. 2010, pp. 1558–1562.
[8] A.K. Khandani, Full-duplex (two-way) wireless: Antenna design and signal processing, [online] Available: ⟨http://www.cst.uwaterloo.ca/reports/antenna_design.pdf⟩, 2012.

[9] W. Cheng, X. Zhang, H. Zhang, Optimal dynamic power control for full-duplex bidirectional-channel based wireless networks, in: Proceedings IEEE INFOCOM'13, Turin, Italy, Apr. 2013, pp. 3120–3128.
[10] D.P. Palomar, M. Chiang, A tutorial on decomposition methods for network utility maximization, IEEE J. Sel. Areas Commun. 24 (8) (2006) 1439–1451.
[11] M. Chiang, Balancing transport and physical layers in wireless multihop networks: jointly optimal congestion control and power control, IEEE J. Sel. Areas Commun. 23 (1) (2005) 104–116.
[12] J. Papandriopoulos, J.S. Evans, Low-complexity distributed algorithms for spectrum balancing in multi-user DSL networks, in: Proceedings IEEE ICC'06, Istanbul, Turkey, June 2006, pp. 3270–3275.
[13] C. Wang, E.K. Au, R.D. Murch, W.H. Mow, R.S. Cheng, V. Lau, On the performance of the MIMO zero-forcing receiver in the presence of channel estimation error, IEEE Trans. Wirel. Commun. 6 (March (3)) (2007) 805–810.
[14] J.I. Choi, M. Jain, M,K. Srinivasan, P. Levis, S. Katti, Achieving single channel, full duplex wireless communication, in: Proceedings ACM MobiCom/MobiHoc'10, Chicago, IL, Sept. 2010, pp. 1–12.
[15] D. Bharadia, E. McMilin, S. Katti, Full duplex radios, in: Proceedings ACM SIGCOMM 2013, Hong Kong, China, Aug. 2013, pp. 375–386.
[16] A. Sabharwal, P. Schniter, D. Guo, D. W. Bliss, S. Rangarajan, R. Wichman, In-band full-duplex wireless: challenges and opportunities, in: IEEE J. Sel. Areas Commun., vol. 32, no. 9, pp. 1637–1652, Sept. 2014.
[17] S. Chen, M. Beach, J. McGeehan, Division-free duplex for wireless applications, IEEE Electron. Lett. 34 (January (2)) (1998) 147–148.
[18] N. Tang, S. Mao, S. Kompella, Power control in full duplex underlay cognitive radio networks: A control theoretic approach, in: Proceedings IEEE MILCOM'14, Baltimore, MA, Oct. 2014, pp. 949–954.
[19] M. Feng, S. Mao, T. Jiang, Duplex mode selection and channel allocation for full-duplex cognitive femtocell networks, in: Proceedings IEEE WCNC 2015, New Orleans, LA, Mar. 2015, pp. 1900–1905.
[20] M. Feng, S. Mao, T. Jiang, Joint duplex mode selection, channel allocation, and power control for full-duplex cognitive femtocell networks, Elsevier Digit. Commun. Netw. J. 1 (February (1)) (2015) 30–44.